Preparation and superconductivity of iron selenide thin films

Preparation and superconductivity of iron selenide thin films

Y Han, W Y Li, L X Cao[1], S Zhang, B Xu and B R Zhao

National Laboratory for Superconductivity, Institute of Physics and Beijing National
Laboratory for Condensed Matter Physics, Chinese Academy of Sciences, Beijing 100190,
People's Republic of China

E-mail: lxcao@aphy.iphy.ac.cn

Abstract
$FeSe_x$ ($x = 0.80, 0.84, 0.88, 0.92$) thin films were prepared on $SrTiO_3$(001) (STO),
$(La, Sr)(Al, Ta)O_3$(001) (LSAT), and $LaAlO_3$(001) (LAO) substrates by a pulsed laser
deposition method. All of the thin films show single-phase and c-axis oriented epitaxial growth,
and are superconducting. Among them, the $FeSe_{0.88}$ thin films show a $T_{c,onset}$ of 11.8 K and a
$T_{c,0}$ of 3.4 K. The upper critical magnetic field is estimated to be 14.0 T.

(Some figures in this article are in colour only in the electronic version)

Since the discovery of $LaFeAsO_{1-x}F_x$ superconductor [1],
progress has been made very rapidly and four kinds of iron-
based superconductors in total have been found [1–10]: (1) F-
doped ROFeAs quaternary compounds (1111 phase, R = La,
Ce, Pr, Nd, Sm, Gd, etc) [1–5], (2) double-FeAs-layered
AFe_2As_2 ternary compounds (122 phase, A = Ca, Sr, Ba,
with or without alkali metal doping) [6, 7], (3) single-FeAs-
layered LiFeAs ternary compounds (111 phase) [8, 9], and
(4) α-FeSe binary compounds (11 phase) [10]. Among
them, α-FeSe is very interesting since it possesses the
simplest crystal structure; in particular, it is the arsenic-free
compound and therefore less toxic in nature in comparison
with the other three kinds of pnictide compounds. For such
superconductors, the superconducting transition temperature
can be enhanced up to 27 K/13.5 K ($T_{c,onset}/T_{c,0}$) under
high pressure [11], and 15.3 K/11.8 K ($T_{c,onset}/T_{c,0}$) via Te
substitution [12, 13]. For experimental research into intrinsic
physical properties [14–16] and device applications [17],
development of high quality epitaxial thin films is necessary.
Therefore attempts have been made to obtain epitaxial and
superconducting arsenide thin films [18–20]. For example,
F-doped LaOFeAs thin films have been made and show an
onset of superconductivity of 11 K [18], while for LaOFeAs
thin film without F doping no superconducting transition was
observed [19]. Hiramatsu *et al* [20] had fabricated Co-doped
$SrFe_2As_2$ thin films which showed a $T_{c,onset}$ of 20 K and a
complete superconducting transition at $\sim$15 K. It should be

indicated that thin films in all these studies regarding the 1111
phase and 122 phase have nearly phase pure epitaxy with minor
impurity phases inside [18–20]. In this paper, we report the
synthesis of iron selenide superconductor $FeSe_x$ ($x = 0.80$,
0.84, 0.88, 0.92) thin films. By pulsed laser deposition, we
obtained single-phased, c-axis oriented epitaxial films. The
films show a $T_{c,onset}$ of 11.8 K and a $T_{c,0}$ of 3.4 K with $x =
0.88$. The upper critical field is estimated to be 14.0 T.

The thin films were pulsed laser deposited in a vacuum
chamber with base pressure better than 4×10^{-5} Pa. An
XeCl excimer laser (308 nm wavelength) with a repetition
rate of 2 Hz and power density of 100 mJ mm^{-2} was used to
irradiate a polycrystalline $FeSe_x$ ($x = 0.80, 0.84, 0.88, 0.92$)
target, which was sintered twice at 600 °C for 24 h in vacuum
sealed quartz tubes after the mixtures of Fe and Se powders
were thoroughly ground. The x-ray diffraction (XRD) pattern
of one such prepared target ($x = 0.88$) and also its R–T
and M–T measurement results ($x = 0.88$) are reproduced
in figure 1(a) and figure 2(a), respectively. It can be seen
that the main synthesis product is tetragonal α-FeSe with the
minor impurity hexagonal β-FeSe, indicated by a star symbol
for its strongest diffraction line; cf figure 1(a). From its R–T
measurement, the zero-resistance temperature is 5.2 K and the
onset temperature is 14.4 K; from its M–T measurement, the
transition temperature is 7.9 K, as shown in figure 2(a).

It is worthy of note that plotting the XRD intensity
on a logarithmic scale is common for identifying and for
recognizing the weaker diffraction peaks, rather than plotting
on a linear scale. The humps of about 200 cps in intensity for

---

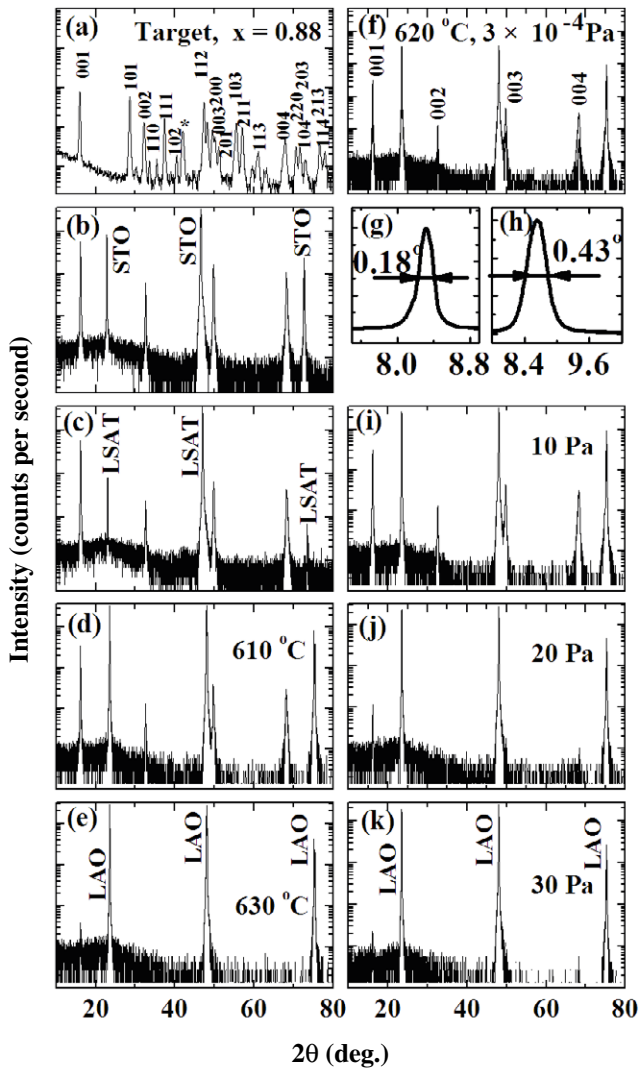[1] Author to whom any correspondence should be addressed.

Figure 1. X-ray diffraction spectra of FeSe$_{0.88}$: (a) target, (b) film on STO at 620 °C under 3×10^{-4} Pa, (c) film on LSAT at 620 °C under 3×10^{-4} Pa, (d) film on LAO at 610 °C under 3×10^{-4} Pa, (e) film on LAO at 630 °C under 3×10^{-4} Pa, (f) film on LAO at 620 °C under 3×10^{-4} Pa, (i) film on LAO at 620 °C under 10 Pa, (j) film on LAO at 620 °C under 20 Pa, and (k) film on LAO at 620 °C under 30 Pa. Rocking curves of the (001) peaks of the films given in (f) and (i) are reproduced in (g) and (h), respectively.

small diffraction angles (10°–30°) are artifacts arising from the diffractometer.

The deposition procedure and parameters were studied and optimized systematically for all four nominal compositions, namely, $x = 0.80$, 0.84, 0.88, and 0.92, for over 150 thin film samples on three kinds of substrates, i.e., SrTiO$_3$(001) (STO), (La, Sr)(Al, Ta)O$_3$(001) (LSAT), and LaAlO$_3$(001) (LAO). The films given in this paper are all about 200 nm thick.

In general, it was found that the pure single-phased, c-axis oriented FeSe$_x$ films can be obtained on all three kinds of substrates, as given in figures 1(b) and (c) for those on STO and LSAT, respectively. The deposition parameters of these two films are the same as those for the best films grown on LAO (cf figure 1(f)), the details of which will be given later.

Since the lattice mismatch is the smallest for FeSe$_x$ films on LAO and also since the physical properties are much better for films on LAO than on STO and LSAT, we concentrate on the LAO cases.

For films with $x = 0.88$ deposited on LAO under different conditions, some of their XRD patterns are given in figures 1(d)–(k) as examples. From the crystal structure point of view, the pure single-phased, c-axis oriented FeSe$_x$ films can be obtained for relatively large ranges of deposition pressure and temperature, e.g. from several tenths of a pascal down to vacuum deposition, and from 630 down to 500 °C; cf figure 2(b), a phase diagram. It is obvious that the films deposited at 620 °C under 3×10^{-4} Pa, i.e., vacuum deposition without argon gas intentionally let into the chamber, show the best crystalline quality among all samples studied (cf figure 1(f)). For example, the full widths of half-maximum of the rocking curves of the FeSe$_{0.88}$(001) diffraction peak are 0.18° and 0.43° (cf figures 1(g) and (h)), respectively, for films deposited under vacuum (cf figure 1(f)) and 10 Pa (cf figure 1(i)), both at 620 °C. It is interesting to note that usually some kinds of gases are intentionally introduced into the deposition chamber in order to adjust and to control the plume of the pulsed laser deposition, in many studies Ar. In this study, it was found that being with or without Ar does influence the quality of the films, which may call for further studies concerning the detailed information on microstructures and/or homogeneities of the structural and electronic phase(s).

However, the physical properties of the films are not that tolerant of deposition conditions in comparison with their crystal structure. Thin films with good superconducting transitions can only be obtained in a relatively small area of the phase diagram, as shown in figure 2(b). As shown in figures 2(c) and (d), the best performance for superconductivity appears at around 620 °C and 3×10^{-4} Pa, with $T_{c,onset}/T_{c,0}$ of 11.8 K/3.4 K. This is in accordance with the above crystal structure studies (cf figures 1(f) and (g)).

The surface morphologies of the films shown in figures 1(d)–(f) and 2(c) were observed with a scanning electron microscope (SEM). The results are reproduced in figure 3; it is a bit surprise that the morphologies are quite different although all other parameters are the same, including the composition, deposition pressure, cooling procedure, etc, with only minor changes in deposition temperature. The film deposited at 610 °C under 3×10^{-4} Pa is quite smooth, showing a featureless surface, which suggests a Frank–van der Merwe growth mode (cf figure 3(a)); while the film deposited at 630 °C shows a Stranski–Krastanov growth mode (cf figure 3(c)). For film deposited at 620 °C, which shows the best qualities in both structure and superconductivity, the surface features just lie in between the ones at 610 and 630 °C: either Frank–van der Merwe growth with nanometer-scale dots precipitated on the surface or an early stage of Stranski–Krastanov growth (cf figures 3(b) and (d)). However, it possesses microcracks which are ∼1 μm away from each other and are aligned along the principal axes of LAO, i.e., [100] or [010]. This may result from the difference in crystalline structure between the LAO and FeSe$_x$, the former of which is pseudo-cubic and the later tetragonal. The minor lattice distortion originating from
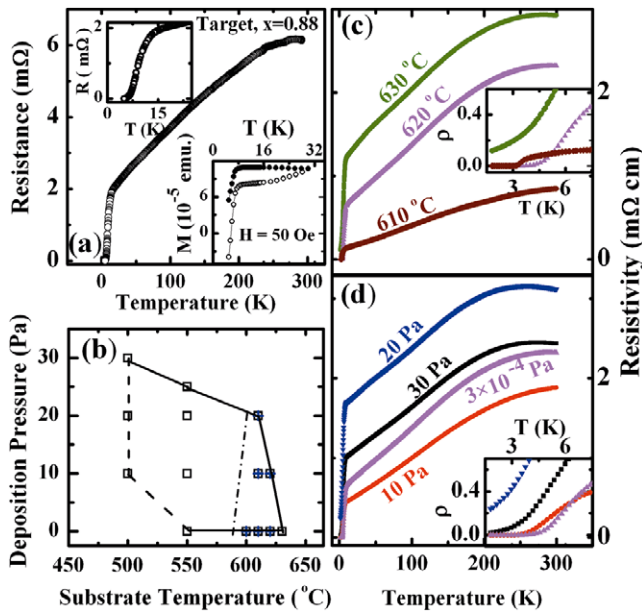
Figure 2. (a) Dependence of the resistance and magnetization (lower right inset) on temperature for the FeSe$_{0.88}$ target pellet, with the upper left inset an enlargement of the R–T curve. (b) Phase diagram of FeSe$_{0.88}$ film deposition, with the empty square labeling which pure single-phased epitaxial films could be obtained, and the cross symbol, superconductivity detected. (c) Resistivity versus temperature for FeSe$_{0.88}$ film on LAO deposited under 3×10^{-4} Pa at different temperatures. (d) Resistivity versus temperature for FeSe$_{0.88}$ film on LAO deposited at 620 °C under different pressures.
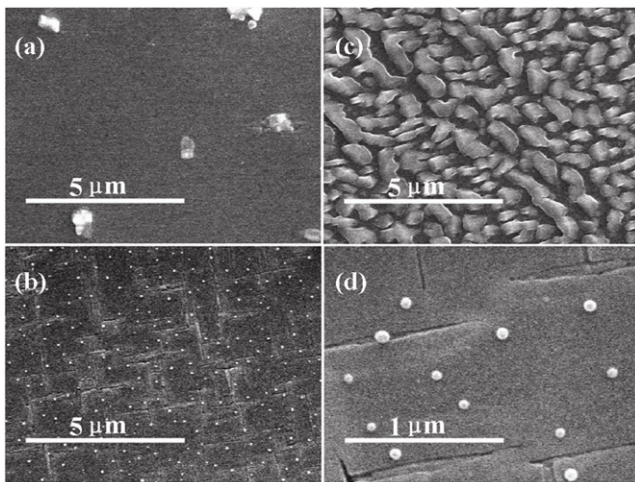

Figure 3. SEM pictures of FeSe$_{0.88}$ films on LAO(001) deposited under 3×10^{-4} Pa at (a) 610 °C, (b) 620 °C, and (c) 630 °C. (d) Same surface as in (b), with higher magnification.

the shear strain determines the critical thickness and the film microstructures [21]. Furthermore, the phase transitions for LAO at ∼435 °C and for α-FeSe at 457 °C may also influence the microstructure and morphology of the films.

The superconducting features of the FeSe$_x$ thin films with $x = 0.80$, 0.84, 0.88, and 0.92 are shown in figure 4(a), in which the superconducting transition temperatures are summarized. It looks to have a dome-like feature with the
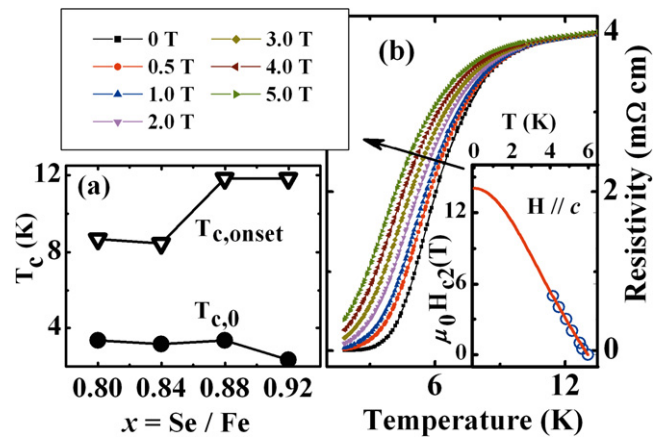

Figure 4. (a) Dependence of $T_{c,onset}$ and $T_{c,0}$ on the Se content for films deposited on LAO at 620 °C under 3×10^{-4} Pa. (b) Resistivity versus temperature in the external magnetic field. The zero-temperature upper critical field is ∼14.0 T, as given in the inset of panel (b).

highest critical temperature at $x = 0.88$. Therefore, we further made a study on the influence of magnetic field on superconductivity for FeSe$_{0.88}$ thin films which are deposited at 620 °C under 3×10^{-4} Pa. For this, magnetic fields up to 5 T are applied along the c-axis, and the R–$T(H)$ data are shown in figure 4(b). The transition curve shifted to lower temperature while the field increased. As shown in figure 4(b), it can be seen that like for the cuprate superconductor, the onset superconducting transitions are the same for all testing magnetic fields, and the broadening of the superconducting transition occurs with increasing magnetic field. This implies a mode of vortex motion similar to that for cuprate superconductor. By using the middle point of the superconducting transition temperature to determine T_c for each field, the upper critical field $H_{c,2}(0)$ can be estimated to be 14.0 T according to the WHH model [22], as shown in the inset of figure 4(b). This value is close to that obtained from the polycrystalline samples [10].

In summary, we deposited pure iron-based superconducting thin films, in particular, c-oriented iron selenide FeSe$_x$ films, on STO, LSAT, and LAO, with $x = 0.80$, 0.84, 0.88, and 0.92. For $x = 0.88$, the films on LAO show $T_{c,onset}/T_{c,0}$ of 11.8 K/3.4 K, and $H_{c,2}$ of 14.0 T.

Acknowledgments

References

[1] Kamihara Y, Watanabe T, Hirano M and Hosono H 2008 *J. Am. Chem. Soc.* **130** 3296
[2] Takahashi H, Igawa K, Arii K, Kamihara Y, Hirano M and Hosono H 2008 *Nature* **453** 376
[3] Chen X H, Wu T, Wu G, Liu R H, Chen H and Fang D F 2008 *Nature* **453** 761

[4] Chen G F, Li Z, Wu D, Li G, Hu W Z, Dong J, Zheng P, Luo J L and Wang N L 2008 *Phys. Rev. Lett.* **100** 247002

[5] Ren Z A, Lu W, Yang J, Yi W, Shen X L, Li Z C, Che G C, Dong X L, Sun L L, Zhou F and Zhao Z X 2008 *Chin. Phys. Lett.* **25** 2215

[6] Rotter M, Tegel M and Johrendt D 2008 *Phys. Rev. Lett.* **101** 107006

[7] Sasmal K, Lv B, Lorenz B, Guloy A M, Chen F, Xue Y Y and Chu C W 2008 *Phys. Rev. Lett.* **101** 107007

[8] Wang X C, Liu Q Q, Lv Y X, Gao W B, Yang L X, Yu R C, Li F Y and Jin C Q 2008 arXiv:0806.4688

[9] Tapp J H, Tang Z, Lv B, Sasmal K, Lorenz B, Chu P C W and Guloy A M 2008 *Phys. Rev.* B **78** 060505

[10] Hsu F C, Luo J Y, Yeh K W, Chen T K, Huang T W, Wu P M, Lee Y C, Huang Y L, Chu Y Y, Yan D C and Wu M K 2008 *Proc. Natl Acad. Sci.* **105** 14262 arXiv:0807.2369

[11] Mizuguchi Y, Tomioka F, Tsuda S, Yamaguchi T and Takano Y 2008 *Appl. Phys. Lett.* **93** 152505

[12] Yeh K W, Huang T W, Huang Y L, Chen T K, Hsu F C, Wu P M, Lee Y C, Chu Y Y, Chen C L, Luo J Y, Yan D C and Wu M K 2008 arXiv:0808.0474

[13] Mizuguchi Y, Tomioka F, Tsuda S, Yamaguchi T and Takano Y 2008 arXiv:0811.1123

[14] Tsuei C C, Kirtley J R, Rupp M, Sun J Z, Gupta A, Ketchen M B, Wang C A, Ren Z F, Wang J H and Bhushan M 1996 *Science* **271** 329

[15] Gozar A, Logvenov G, Kourkoutis L F, Bollinger A T, Giannuzzi L A, Muller D A and Bozovic I 2008 *Nature* **455** 782

[16] Zhao B R 2002 Superconductor thin films *Handbook of Thin Film Materials* vol 4, ed H S Nalwa (San Diego, CA: Academic) pp 507–624

[17] Gupta A A, Sun J Z and Tsuei C C 1994 *Science* **265** 1075

[18] Backen E, Haindl S, Niemeier T, Freudenberg T, Werner J, Behr G, Schultz L and Holzapfel B 2008 arXiv:0808.1864

[19] Hiramatsu H, Katase T, Kamiya T, Hirano M and Hosono H 2008 *Appl. Phys. Lett.* **93** 162504

[20] Hiramatsu H, Katase T, Kamiya T, Hirano M and Hosono H 2008 *Appl. Phys. Express* **1** 101702 arXiv:0808.1985

[21] Cao L X, Lee T L, Renner F, Su Y, Johnson R L and Zegenhagen J 2002 *Phys. Rev.* B **65** 113402

[22] Fang L, Wang Y, Zou P Y, Tang L, Xu Z, Chen H, Dong C, Shan L and Wen H H 2005 *Phys. Rev.* B **72** 014534